JOURNAL OF MATERIALS SCIENCE 37 (2002) 801 – 806

Synthesis and characterization of CuO containing mesoporous silica spheres

LIANZHOU WANG,*,‡ S. VELU, S. TOMURA, F. OHASHI, K. SUZUKI, M. OKAZAKI, T. OSAKI, M. MAEDA
Ceramic Research Institute, Chubu Center, National Institute of Advanced Industrial Science and Technology, 1-1 Hirate, Kita-ku, Nagoya 462-8510, Japan
E-mail: wang.lianzhou@nims.go.jp

A new series of mesoporous silica spheres containing nanodispersed copper oxides were synthesized in H_2O/EtOH/ammonia solution at room temperature. The mesoporous structures were characterised using X-ray powder diffraction and N_2 adsorption-desorption techniques. Scanning electron micrograph and transmission electron micrograph revealed that the MCM-41 particles have spherical morphologies. The DTA curve of pure MCM-41 exhibited a sharp single exothermic peak between 290°C and 340°C, while a broad peak with several shoulders in the temperature range between 180°C and 380°C was observed for Cu-MCM-41, indicating the possible complexation of Cu^{2+} with surfactants adhering to the inner surfaces of the mesopores. Electron paramagnetic resonance spectra of uncalcined samples revealed that Cu^{2+} ions are in an octahedral or distorted octahedral coordination with nitrogen ligands of the surfactant while in the calcined samples they are coordinated with oxygen of the MCM-41 framework. The redox properties of samples were examined by a temperature-programmed reduction and N_2O passivation method. The results indicate that CuO with increasing particle size could be formed in the mesoporous materials with increasing Cu contents, and this decreased the reducibility of the resulting CuO.

1. Introduction

Since the scientists of Mobil Corp. reported their pioneering work on silica-based mesoporous materials, designated as M41S [1, 2], considerable research effort has been made in this area [3–6]. The M41S materials possess a regular array of uniform nanostructured pores, which can be systematically varied from around 15 to 100 Å in diameter. These characteristics, together with their extraordinary high surface area and distinct adsorption properties, open up many potential applications in catalysis, separation, nano-technology, etc.

Many modifying elements such as Al [1, 7, 8], Ti [9, 10], V [11], Fe [12], B [13], Ga [14], Zr [15], and Mn [16], etc., have been incorporated into mesoporous silica to generate catalytic activity. Since it is well known that Cu ions show redox properties, Cu-containing mesoporous silica materials have been the subject of recent research [17–20]. Owing to the difficulty of introducing divalent metals into a tetravalent silicon framework, most of the work has focused on the classical two-step method of ion-exchange [18, 20], grafting [19] or impregnation [21] to introduce Cu ions into tetravalent or trivalent metal ion modified mesoporous silica materials. Recently, the direct co-assembly of Cu ions with silicon precursors using complexes of Cu with suitable organofunctional silicon alkoxides [22, 23], has provided new pathways for the synthesis of these mesoporous materials.

In the present work, a simple way to rapidly synthesize CuO containing MCM-41 spherical particles in a H_2O/EtOH/ammonia system at room temperature is presented. It is well known that transition metal ions, such as Cu^{2+}, can combine with NH_4^+ to form coordinated complex cations. Thus, the employment of ammonia avoids the precipitation of Cu in a basic solution. The CuO containing mesoporous materials prepared in this way are spherical. The dispersion and redox properties of these materials are investigated using a temperature-programmed reduction and N_2O passivation method.

2. Experimental procedure

2.1. Materials synthesis

Mesoporous silica samples with different amounts of divalent Cu ions were rapidly synthesized at room temperature. Aqueous solutions of hexadecyltrimethylammonium (C_{16}TMACl), ammonia, tetraethylorthosilicate (TEOS) and different amounts of $Cu(CH_3COO)_2$ were well mixed to obtain a gel with molar composition of $0.25C_{16}TMACl : 1TEOS : 8NH_4OH :$

*Author to whom all correspondence should be addressed.
‡*Present Address*: Advanced Materials Lab., National Institute for Materials Science, 1-1 Namiki, Tsukuba, Ibaraki 305-0044.

$160H_2O : 50EtOH : x$ $Cu(CH_3COO)_2$, with x in the range 0 to 0.08. In a typical synthesis procedure, 1.31 g of C_{16}TMACl was added to the mixed solution of 50 ml of H_2O and 47.5 ml of EtOH; 8.5 ml of NH_4OH (28% aqueous solution) containing 0.03 g of $Cu(CH_3COO)_2 \cdot H_2O$ were added into the homogenous solution, giving rise to a dark blue solution; 3.64 ml of TEOS was introduced. After stirring for 2 hours, the blue products were filtered, washed with distilled water and heated in an oven at 75°C. The as-synthesized samples were calcined in air at 540°C for 18 hours to obtain light-blue colored copper containing MCM-41 materials.

2.2. Characterization

The X-ray powder diffraction (XRD) measurements of samples were carried out on a Rigaku RINT 2000 X-ray diffractometer with Cu K_α radiation. The chemical compositions of the samples were determined by X-ray fluorescence spectroscopy (XFS) (MESA-500NA). N_2 adsorption isotherms were measured at 77 K using a Sorptomatic 1900 analyzer. The volume of absorbed N_2 was normalized to standard temperature and pressure (STP). The specific surface area (S_{BET}) of samples was determined from the linear part of BET plot ($P/P_0 = 0.05-0.15$). The pore size distribution (PSD) was calculated using the Barrett-Joyner-Halenda (BJH) formula. Scanning electron micrographs (SEM) were observed on a Hitachi S-3500N instrument. Imaging of the sample was conducted with a JEOL-200 CX transmission electron microscope (TEM) operated at 200 keV. Thermogravimetric Analysis (TGA) was carried out using a Seiko RTG-320U instrument with a heating rate of 2°C/min in air. Electron paramagnetic resonance (EPR) spectra of samples were recorded on a JEOL EPR spectrometer (JES-RE1XM) operating in the X-band region. The microwave power was 3.0 mV, and the amplitude of magnetic field modulation at 100 kHz was 0.03 mT. Observation was made both at room temperature (≈298 K) and at 77 K. About 40 mg of the sample was taken in a 4 mm o.d. quartz tube, evacuated to ca. 10^{-3} Torr. The tube was sealed under vacuum after introducing ca. 10 Torr He gas and then set in the quartz dewar vessel in the EPR cavity. A sample of diphenylpicrylhydrazyl (DPPH; $g = 2.0037$) was used as a reference to mark the g-value. Simulation of the observed spectra (77 K) was made assuming g-and hyperfine coupling tensors with axial symmetry.

The reducibility and the CuO particle sizes of Cu containing MCM-41 samples were determined by temperature-programmed reduction (TPR) and the N_2O passivation method [24, 25]. About 50 mg of the calcined sample was placed in a quartz reactor and heated under a reducing flow of H_2 (5 vol% in Ar) at a heating rate of 5°C/min up to 500°C. The hydrogen consumption due to the reduction of CuO was determined continuously using a gas chromatograph (Shimadzu GC-8A). Hydrogen consumption was calculated quantitatively from the TPR peak area, calibrated with a standard CuO sample. A normal TPR was conducted first by heating the sample from room temperature to 500°C and then the sample was cooled to 60°C and ventilated with He instead of H_2 for about 15 min. Afterwards, the sample was exposed to pure N_2O flow at 60°C to passivate the samples for 1 h. Finally, the samples were purged with He again to eliminate the residual oxidant and a second TPR was recorded to assess the amount of oxygen by the chemisorption of N_2O on the surface of Cu metal.

3. Results and discussion

3.1. XFS and XRD results

The chemical compositions of Cu-containing samples were determined by XFS and the results were shown in Table I.

For calcined Cu-MCM-41 materials, the variations in the peak intensities in the XRD patterns were recorded (See Fig. 1). A rather intense diffraction (100) peak between $2\theta = 2$–3° was recorded for each sample with Cu ≤ 3.02 wt%. Additional (110) and (200) peaks around $2\theta = 3$–6°, which are usually observed in ordered MCM-41 materials [1], were also observed in these samples, indicating that the samples could be rapidly synthesized at room temperature. However, (100) peak intensities of samples with higher Cu contents (samples C3 and C4) were relatively weak, indicating that a certain amount of Cu-doping could lead to the collapse of ordered porous framework in MCM-41 materials.

3.2. TGA-DTA results

The thermogravimetric analysis results of uncalcined MCM-41 samples are shown in Fig. 2. Each curve shows two or three major weight loss steps and then the sample experiences no further weight loss. The first weight loss below 180°C is due to desorption of physically absorbed water. A prominent weight loss appears between 180°C and 380°C and can be assigned to the decomposition of surfactants during combustion. The final small weight loss above 380°C is associated with continuing polymerization of a few remaining silanol groups in the framework. The pure silica sample, P0, has the largest weight loss of 52.70%, and the losses of Cu-MCM-41 materials decrease with increasing Cu-content. This implies that the amounts of

TABLE I Chemical composition and microstructural parameters of samples

Sample	CuO (wt%)	d_{100} (Å)	S_{BET} (m^2/g)	Pore diameter (Å)	Pore volume (cm^3/g)
P0	0	34.6	1629	22.8	0.835
C1	0.54	33.7	1646	22.4	0.804
C2	1.26	34.9	1403	23.8	0.799
C3	3.02	35.5	1252	23.6	0.653
C4	5.28	37.1	538	21.8	0.293

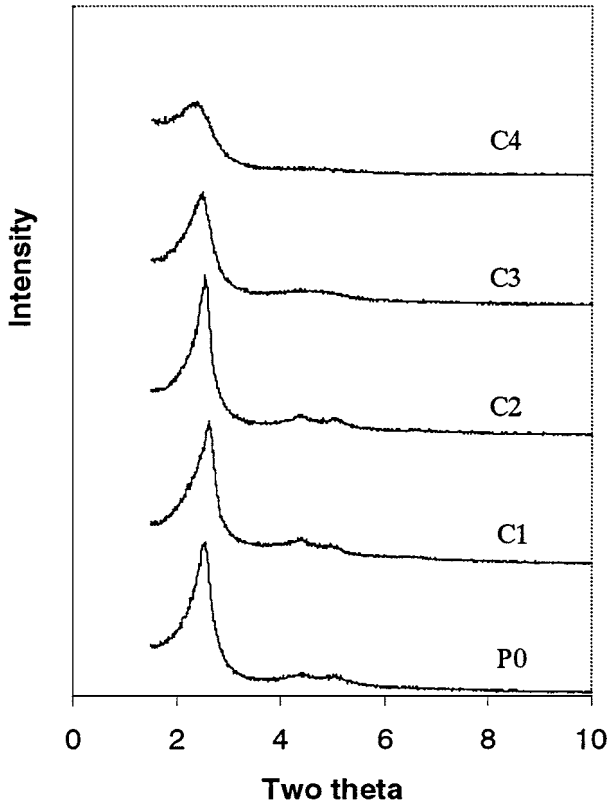

Figure 1 XRD patterns of the Cu-MCM-41 materials. (Calcined at 540°C).

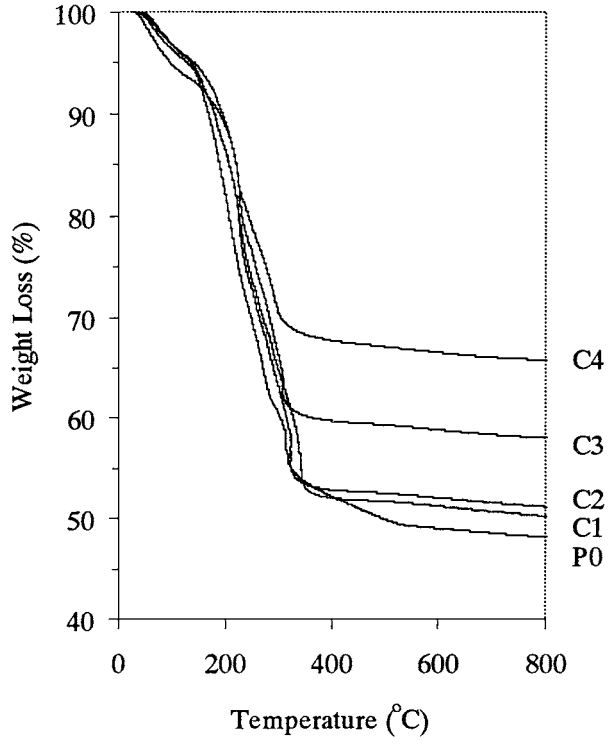

Figure 2 TGA weight loss curves of Cu-MCM-41 materials.

surfactant in the Cu-MCM-41 samples are less than those in the pure silica sample. It is also interesting to note that the DTA curves of Cu-MCM-41 materials are significantly different from that of the pure silica sample P0 (Fig. 3). The latter sample (P0) exhibits a sharp exothermic signal, which is associated mainly with the combustion and decomposition of organic surfactants. On the other hand, the Cu-MCM-41 materials exhibit a

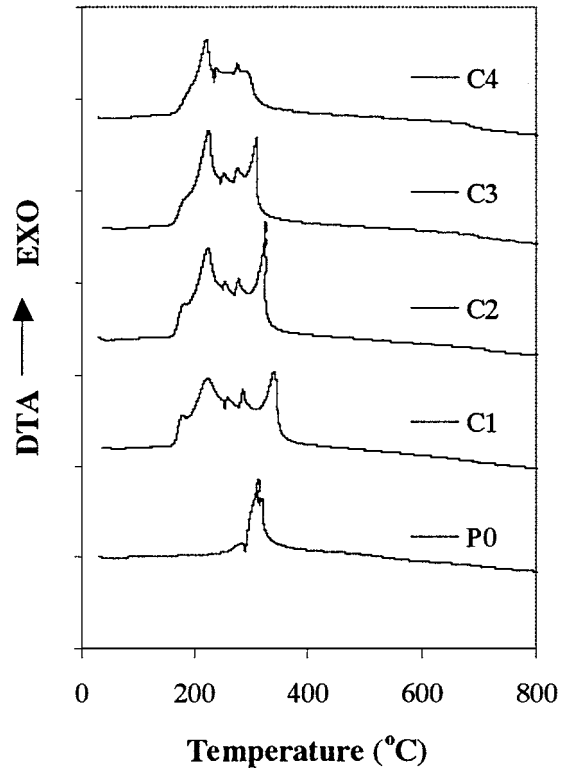

Figure 3 DTA curves of Cu-MCM-41 materials.

broad exothermic peak with several shoulders between 180–380°C. If Cu ions were buried in the framework of silica, then the rather small amounts of Cu ions in these samples could not contribute to the significant difference in the thermal behavior as identified by DTA. Therefore, it is suggested that the Cu ions are located on the inner surfaces of mesopores, where they might combine with surfactant molecules to form some metal-organic complexes. As a result, the combustion and decomposition behavior of surfactants in these materials is influenced significantly by the presence of Cu ions.

3.3. N_2 adsorption isotherms and pore size distributions

The nitrogen adsorption isotherms of samples are shown in Fig. 4 and the parameters derived from these isotherms are listed in Table I. It can be seen that in all cases, with the exception of sample C4, the isotherms belong to the type IV, typical mesoporous solids. A well-defined step occurs in those isotherms between $P/P_o = 0.15$ and 0.3, which is characteristic of capillary condensation of N_2 molecules in the uniform mesopores of MCM-41 materials. However, the deleterious effects of metals ions introduced to mesoporous silica materials are well illustrated by the amounts of N_2 adsorbed. The isotherm of sample C4 has already lost the characteristic mesoporous solid shape and its specific surface area decreased sharply to 538 m^2/g. The pore size distribution curves (Fig. 5) show that most samples have narrow size distributions of mesopores; meanwhile, sample C4 has a wider pore size distribution and the smallest BJH differential pore volume (Dv/Dr), suggesting that the framework of mesoporosity is not uniform, which is consistent with the results of XRD.

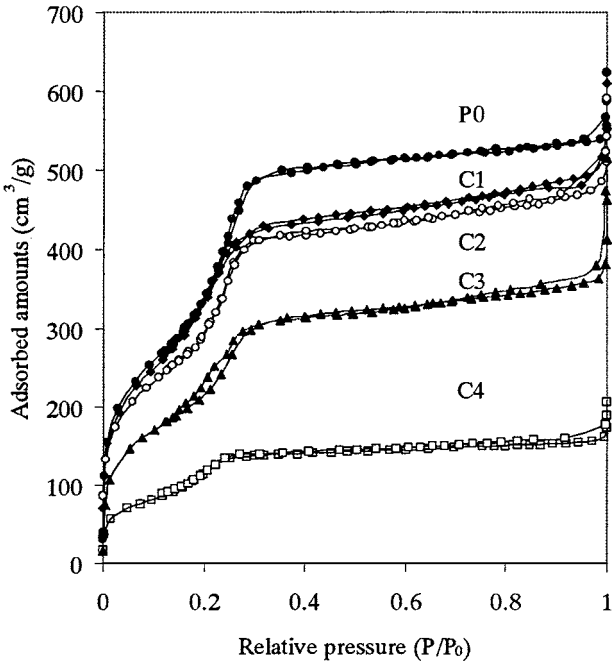

Figure 4 Nitrogen adsorption-desorption isotherms of Cu-MCM-41 materials.

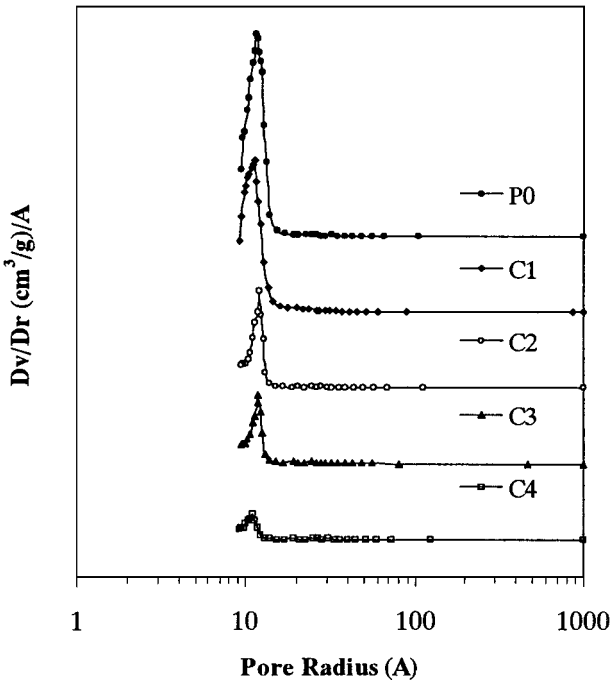

Figure 5 BJH differential pore size distributions of Cu-MCM-41 materials.

3.4. SEM and TEM

Recently, many efforts have been focused on the self-assembly of mesoporous materials with particular morphologies. Many unusual shapes, such as discoids, gyroids, hollow tubular, hexagonal prism and spheres have been successfully synthesized [26–28]. From the SEM image of sample C2 (Fig. 6), it can be seen that the morphology of the sample is principally spherical. If the samples were synthesized in aqueous solution without the addition of EtOH, the morphologies of the materials were not sphere-like any more. From the high-resolution TEM image of calcined sample C2 (Fig. 7), a well-ordered hexagonal arrangement of nanosized mesopores can be seen in the spherical particles.

3.5. Electron paramagnetic resonance spectroscopy

EPR spectroscopy is a powerful method to explore the chemical environments of Cu^{2+} ions in the MCM-41 materials. The spectra of uncalcined and calcined samples were recorded at 77 K. It can be seen (Fig. 8) that the uncalcined sample C2 containing about 1.26 wt% of CuO exhibits four well-resolved hyperfine lines ($m_I = -3/2, -1/2, +1/2, +3/2$), which are characteristic of a copper nucleus with $I = 3/2$, both in the parallel and perpendicular regions of the spectrum. For sample C4, containing about 5.28 wt% of CuO, the perpendicular part of the spectrum is poorly resolved because of the high surface concentration of Cu^{2+} ions. The line width of the hyperfine component at higher field is larger than that of the component at lower field. This effect has been attributed to the distributions of g- and A-tensors, whose components are correlated to each other. These distributions are as a result of a difference in the microenvironment of the paramagnetic center [29, 30].

The spin Hamiltonian parameters, g and A have been extracted by the simulation of spectra recorded at 77 K. The EPR spectra of uncalcined sample C2 exhibits a single copper species, which can be described by the spin Hamiltonian parameters $g_{\|} = 2.287$, $g_{\perp} = 2.048$, $A_{\|} = 164$ G and $A_{\perp} = 24$ G. The g and A values of uncalcined C4 are similar to those of sample C2. It has been reported that the parameter set, $g_{\|} = 2.24$ and $A_{\|} = 163$ G, which often indicates a square planar coordination, is observed for octahedral Cu^{2+} complexes involving nitrogen ligands [17]. Therefore, the observed spin Hamiltonian parameters of the uncalcined samples are attributed to Cu^{2+} ions in an octahedral or distorted octahedral coordination with nitrogen ligands of the surfactant, which supports the assumption that Cu ions might locate on the inner surfaces of mesopores.

Compared with the results of uncalcined samples, the spectra of calcined samples are significantly different (Fig. 8). The perpendicular parts of the spectrum are poorly resolved while the resolution in the parallel part of the spectrum is improved. In addition, the $g_{\|}$ value increases while $A_{\|}$ decreases. The spectrum of CuMCM-41 containing 1.26 wt% of CuO can be described with the spin Hamiltonian parameters $g_{\|} = 2.383$, $g_{\perp} = 2.068$, $A_{\|} = 123$ G and $A_{\perp} = 10$ G. These values are very close to those reported for $[Cu(H_2O)_6]^{2+}$ found in the hydrated ion-exchanged CuMCM-41 materials [17]. Hence, the chemical environment of Cu^{2+} ions might be an octahedral or elongated octahedral coordination with oxygen of the MCM-41 framework. The larger line width of calcined samples compared with their uncalcined counterparts implies that the structure around the Cu^{2+} ion is randomized upon calcination, probably because of the change in the coordinating ligand from nitrogen (strong field) in the uncalcined samples to oxygen (weak field) in the calcined samples. Thus, the change in the spectral

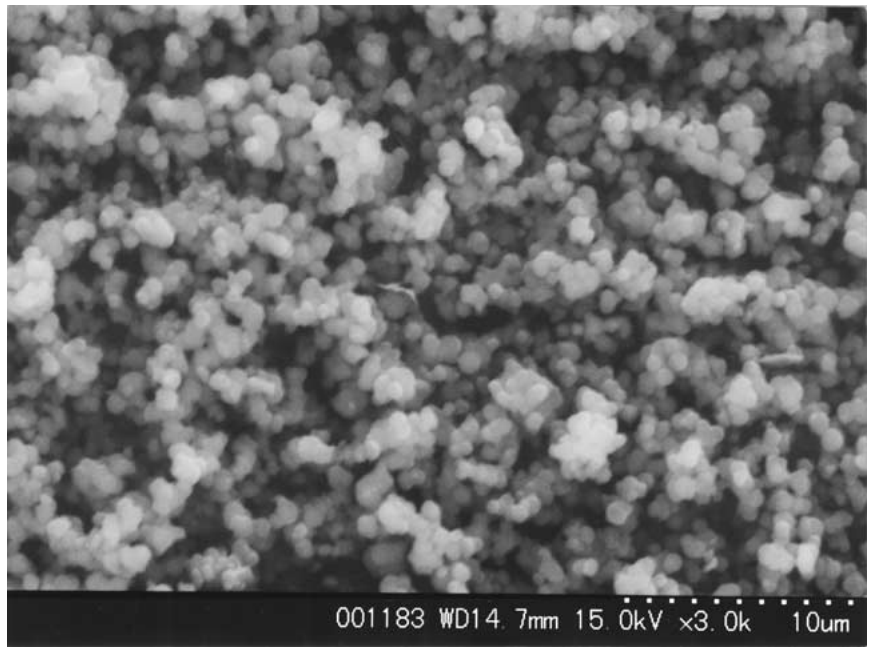

Figure 6 SEM image of sample C2.

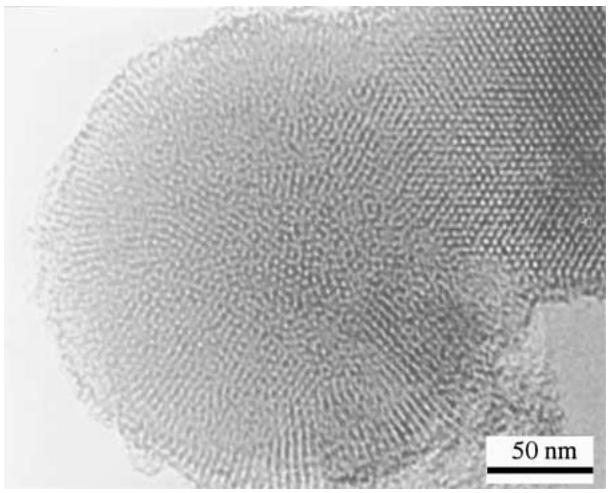

Figure 7 High-resolution TEM image of sample C2.

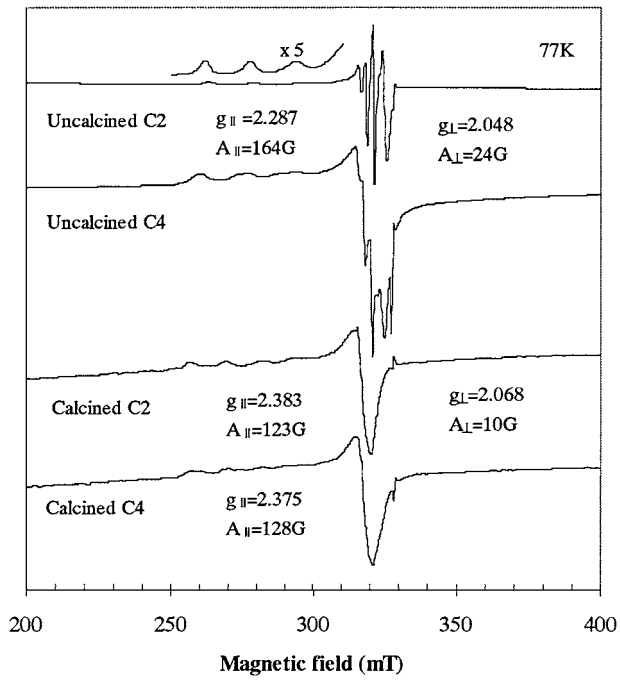

Figure 8 Electron Spin Resonance spectra of uncalcined and calcined CuMCM-41 materials recorded at 77 K.

pattern with concomitant increase in $g_{\|}$ value and decrease in $A_{\|}$ value compared with the uncalcined sample is as a result of a complete substitution of nitrogen ligands by framework oxygen. Similar results have also been reported in the EPR characterization of CuMCM-41 synthesized by a sol-gel method [23].

3.6. TPR and N_2O passivation results

TPR have been widely used to assess the redox properties of metal oxide catalysts. In the present work, a TPR together with a N_2O passivation method were employed to quantitatively investigate the particle sizes of CuO dispersed in the Cu-MCM-41 materials. The method is based on the measurement of hydrogen consumption after complete oxidation of Cu-MCM-41 materials and after surface oxidation of the same sample. After the first TPR process, all the Cu oxide in mesoporous silica was reduced from Cu^{2+} to Cu^0, then the materials were exposed to pure N_2O flow at 60°C. N_2O was believed to be chemisorbed onto the surface atoms of Cu particles and partly oxidized [24] them to Cu^+. Then second identical TPR will determine the amount of Cu atoms on the surface of the Cu particles. Therefore, the molar ratio of total and surface Cu atoms of particles will be calculated from the H_2 consumption based on the two TPR pronfiles.

The TPR profiles of Cu-MCM-41 are shown in Fig. 9. From the solid curves, it could be seen that the maximum rate of H_2 consumption increased with increasing Cu contents of the samples. The temperature for maximum H_2 consumption rate (T_{max}) of samples C2 and C3 were 234°C and 236°C respectively. However,

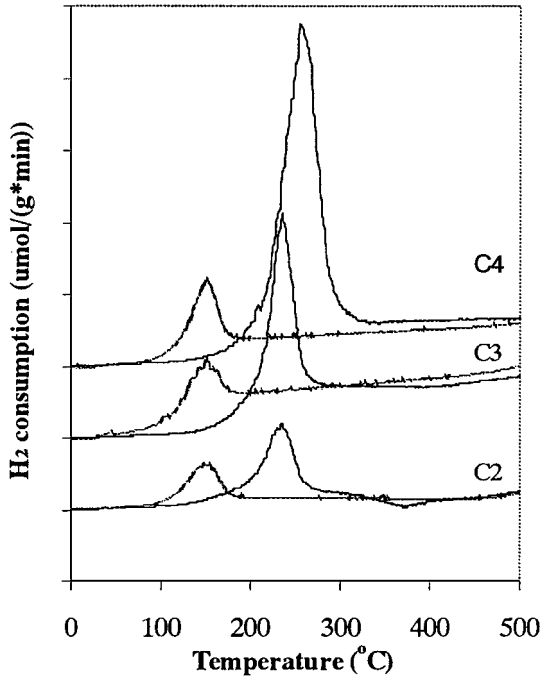

Figure 9 TPR profiles of Cu-MCM-41 materials (Solid lines: first TPR results; dotted lines: second TPR after N_2O passivation).

the T_{max} of C4 shifted to 255°C, about 20°C higher than for C2 and C3. From the TGA-DTA results, it was inferred that the Cu ions probably locate at the interface between the surfactants and the Si-O framework. Upon calcination, the removal of organic species leads to copper oxide adhering to the inner surface of the mesochannels. Therefore, higher amounts of Cu are more likely to aggregate into larger CuO particles and thus, need higher reduction temperatures to reach T_{max} during the TPR [24]. From the dotted lines corresponding to the N_2O-TPR, it can be seen that the T_{max} of all three samples decreases to around 150°C, for the reduction of the surface Cu species (Cu^+). From the areas of the two TPR profiles, the particle sizes of CuO in samples C2, C3 and C4 are found to be 1.35 nm, 1.47 nm and 2.61 nm, respectively. Particles in this size range can be accommodated easily in the mesopores of materials.

XRD was used to determine the particle size of the CuO in the samples, but probably due to the low Cu content of the materials, no peaks corresponding to CuO were found in XRD patterns.

4. Conclusions

Mesoporous silica spheres containing CuO can be synthesized easily in H_2O/EtOH/ammonia solution at room temperature. It has been found from TGA-DTA and EPR experiments that the Cu ions locate on the inner surfaces of the mesopores instead of being buried in the framework of silica. Hence, the Cu^{2+} ions in these materials are expected to have access to foreign molecules passing through the mesopores and can catalyze some oxidation reactions. The CuO particles, of particle size in the range 1.35–2.61 nm, are dispersed within the mesochannels of MCM-41 materials.

Acknowledgements

One of the authors (L. Wang) is deeply appreciative of the Japan International Science and Technology for the award of a STA fellowship.

References

1. C. T. KRESGE, M. E. LEONOWICZ, W. J. ROTH, J. C. VARTULI and J. S. BECK, *Nature* **359** (1992) 710.
2. J. S. BECK, J. C. VARTULI, W. J. ROTH, M. E. LEONOWICZ, C. T. KERSGE, K. D. SCHMITT, C. T. CHU, D. H. OLSEN, E. W. SHEPPARD, S. B. McCULLEN, J. B. HIGGINS and J. L. SCHLENKER, *J. Am. Chem. Soc.* **114** (1992) 10834.
3. Q. HUO, D. MARGOLESE, U. CIESLA, P. FENG, T. E. GIER, P. SIERGER, R. LEAO, P. M. PETROFF, F. SCHUTH and G. D. STUCKY, *Nature* **368** (1994) 317.
4. A. CORMA, *Chem. Rev.* **97** (1997) 2373.
5. J. Y. YING, C. P. MEHNERT and M. S. WONG, *Angew. Chem. Int. Ed.* **38** (1999) 56.
6. K. MOLLER and T. BEIN, *Chem. Mater.* **10** (1998) 2950.
7. Z. H. LUAN, C. F. CHENG, W. Z. ZHOU and J. KLINOWSKI, *J. Phys. Chem.* **99** (1995) 1018.
8. J. AGUADO, D. P. SERRANO and J. M. ESCOLA, *Microporous Mesoporous Mater.* **34** (2000) 43.
9. P. T. TANEV, M. CHIBWE and T. J. PINNAVAIA, *Nature* **368** (1994) 321.
10. K. A. KOYANO and T. TATSUMI, *Chem. Commun.* (1996) 145.
11. K. M. REDDY, I. MONDRAKOVSKI and A. SAYARI, *ibid.* (1994) 1059.
12. B. ECHCHAHED, A. MOEN, D. NICHOLSON and L. BONNEVIOT, *Chem. Mater.* **9** (1997) 1716.
13. A. SAYARI, H. DANUMAH and I. MOUDRAKOVSKI, *ibid.* **7** (1995) 813.
14. C. F. CHENG, H. Y. HE, W. Z. ZHOU, J. KLINOWSKI, J. A. GONCALVES and L. F. GLADDEN, *J. Phys. Chem.* **100** (1996) 390.
15. A. TUEL, S. GONTIER and R. TEISSIER, *Chem. Commun.* (1996) 651.
16. D. ZHAO and D. GOLDFARB, *ibid.* (1995) 875.
17. M. ZIOLEK, I. SOBCZAK and P. NOWAK, *Stud. Surf. Sci. Catal.* **125** (1999) 633.
18. A. POPPL, M. HARTMANN and L. KEVAN, *J. Phys. Chem.* **99** (1995) 17251.
19. V. LUCA, D. J. MACLACHLAN, R. R. BRAMLEY and K. MORGAN, *ibid.* **100** (1996) 1793.
20. J. XU, J. YU, S. J. LEE, B. Y. KIM and L. KEVAN, *J. Phys. Chem.* B **104** (2000) 1307.
21. P. P. PAUL, M. J. HEIMRICH, J. MARTIN and A. MICHAEL, *Catal. Today* **42** (1998) 61.
22. M. A. KARAKASSIDES, K. G. FOURNARIS, A. TRAVLOS and D. PETRIDIS, *Adv. Mater.* **10** (1998) 483.
23. M. A. KARAKASSIDES, A. BOURLINOS, D. PETRIDIS, L. COCHE-GUERÈNTE and P. LABBÈ, *J. Mater. Chem.* **10** (2000) 403.
24. S. VELU, K. SUZUKI and T. OSAKI, *Catal. Lett.* **62** (1999) 159.
25. M. HARTMANN, S. RACOUCHOT and C. BISCHOF, *Chem. Commun.* (1997) 2367.
26. G. A. OZIN, *Acc. Chem. Res.* **30** (1997) 17.
27. H. P. LIN and C. Y. MOU, *Science* **273** (1996) 765.
28. L. Z. WANG, J. L. SH I, F. Q. TANG, J. YU, M. L. RUAN and D. S. YAN, *J. Mater. Chem.* **9** (1999) 643.; L. Z. WANG, S. TOMURA, M. MAEDA, F. OHASHI, K. INUKAI and M. SUZUKI, *Chem. Lett.* (2000) 1414.
29. A. POPPL, M. NEWHOUSE and L. KEVAN, *J. Phys. Chem.* **99** (1995) 10019.
30. P. J. CARL and S. L. BORDIGA, *J. Phys. Chem.* B (104) (2000) 6568.

Received 6 November 2000
and accepted 4 October 2001